

Interconnected Resonant Gyros for Improved Performance

David W. Fogliatti

SPAWAR Systems Center, San Diego
53560 Hull Street
San Diego, CA 92152-5001

ABSTRACT

A brief review of the operation of vibratory gyroscopes and the status of commercial micromachined gyroscopes is presented in the introduction. Following the introduction, an alternative design approach employing multiple, coupled gyroscopes per angular axis is examined as a method to improve performance and redundancy in angular rate sensors. The results are from simulations and explore the effects of non-identical gyroscopes, variations in the driving frequency, and coupling on synchronization in the array. A novel operating approach is presented that requires the array of gyroscopes to be synchronized in phase and frequency to improve the detection of sense axis displacement and to utilize one amplitude demodulator for the entire array of gyroscopes.

1. INTRODUCTION

Vibratory gyroscopes are designed to determine the angular rate of a rotating object. Typically, vibrating gyroscopes can be modeled by the mass spring system shown below in Figure 1.

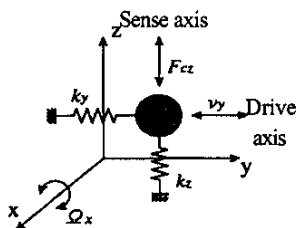


Figure 1. Model for vibratory gyroscope

A mass spring system used to model different types of vibratory gyroscopes.

The operating principle for all vibrating gyroscopes is the transfer of energy from one vibrating mode to another by the Coriolis force. The Coriolis force is an inertial force exerted on a moving body in a rotating reference frame. The gyroscope in Figure 1 has two orthogonal excitation modes with restoring coefficients k_y and k_z . Damping coefficients along each axis (C_y and C_z) are included in the

model. The y-axis mode (drive) is excited by a reference drive force and the z-axis mode (sense) is excited by the Coriolis force (F_{cz}). Displacements along the sense or z-axis are proportional to the applied angular rate Ω_x , if the motion of the drive axis is known. The following equations model this system.

$$m\ddot{y} = -k_y y - C_y \dot{y} + F_{drive} \text{ drive axis} \quad (1a)$$

$$m\ddot{z} = -k_z z - C_z \dot{z} + F_{cz} \text{ sense axis} \quad (1b)$$

$$F_{cz} = \text{Coriolis Force} \quad (1c)$$

$$= |2m \bar{\Omega}_x \times \dot{y}|$$

The critical design issues for micromachined vibratory gyroscopes are detecting sense axis displacements that are orders of magnitude less than the drive amplitude and keeping the drive and sense motions uncoupled. The excitation of the drive mode and displacements along the sense axis are typically measured using electrostatic sensors by applying a voltage or measuring changes in capacitance. The amplitude of the drive axis motion is typically limited to the 1-50 micron range depending on the etching and manufacturing process used. Typical sense axis displacements are orders of magnitude less than drive axis displacements and require sensitive transducers to measure the small displacements. This paper will focus on low cost surface micromachined gyroscopes with capacitive sense axis detection. While capacitive sensors are not ideal for micromachined applications, they can be implemented using standard silicon processing techniques. Micromachined gyroscopes with bias drifts in the 10-50°/h have been produced on a prototype basis [1]. An application for low cost gyroscopes with a 10°/h bias drift is in the automotive industry for roll sensors. Gyroscopes with a bias drift less 0.1°/h are suitable for inertial navigation applications.

2. SIMULATION MODEL

The equations in (1) can be put into a more general form if an amplitude modulated sinusoidal driving force is used to

represent the Coriolis term in the sense axis equation (1b). This simplification requires the drive axis displacement follow a harmonic motion of the form $\cos(\omega_d t)$. This can be accomplished by locking the drive axis displacement to a harmonic reference signal in a gain control loop. Equation (2) describes the sense axis motion (z-axis in figure 1) of the gyroscope using a sinusoidally driven, linearly damped, harmonic oscillator. Equation (3) casts equation (2) in more general terms.

$$m\ddot{z} + C\dot{z} + kz = k\Omega(t)\lambda\sin(\omega_d t) \quad (2)$$

$$\ddot{z} + 2\gamma\dot{z} + \omega_r^2 z = \omega_r^2 \Omega(t)\lambda\sin(\omega_d t) \quad (3)$$

In equation (3) γ is $C/2m$, λ is a constant that includes the drive amplitude, ω_d is the harmonic drive frequency, ω_r is the resonant frequency for the sense axis mode, and $\Omega(t)$ is the angular rotation rate about the x-axis. The general solution for $z(t)$ can be found and it describes the displacement of the sense axis of the gyroscope [2]. Equations (4) and (5) follow from the general solution in the underdamped case where $\gamma < \omega_r$. Z_{\max} describe the maximum amplitude of the sense vibration mode and ϕ is the phase lag of the gyroscope with respect to the driving frequency (ω_d) and the gyroscope sense axis resonant frequency (ω_r).

$$Z_{\max} = \frac{\lambda\Omega(t)}{\sqrt{\left[1 - \left(\frac{\omega_d}{\omega_r}\right)^2\right]^2 + \left[\frac{\omega_d}{\omega_r Q}\right]^2}} \quad (4)$$

$$\phi = \arctan\left[\frac{\frac{\omega_d}{\omega_r Q}}{1 - \left(\frac{\omega_d}{\omega_r}\right)^2}\right], \quad 0 \leq \phi < \pi \quad (5)$$

Q is equal to $\omega_r/(2\gamma)$ and is called the "quality factor" of the sense mode of the gyroscope. Plots of equations (4) and (5) are shown in figure 2.

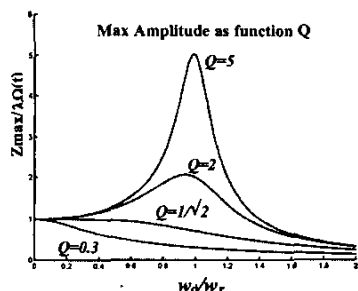


Figure 2a. Plot of Z_{\max} - This figure shows the sharpening of the amplitude response as ω_d approaches ω_r and Q increases.

These equations describe the necessary conditions for the gyroscopes in the array to synchronize and will be used extensively to qualitatively describe the results of the simulations.

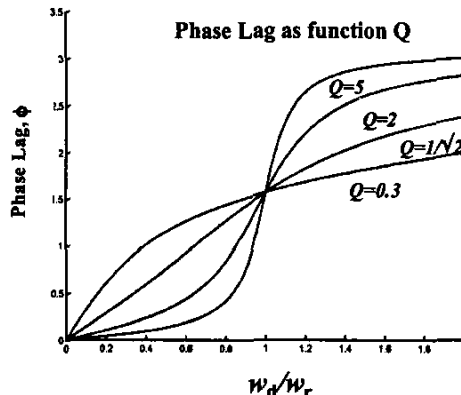


Figure 2b. Plot of Phase Lag, ϕ - This figure shows that for $\omega_r > \omega_d$ the gyroscope will follow the drive frequency with roughly zero phase lag. For $\omega_r = \omega_d$ the sense mode follows the drive frequency by $\pi/2$. For $\omega_d > \omega_r$ the sense mode follows by π . The region of most phase mismatch will be near ω_r and will be worse for high Q .

The main result is that for driving frequencies less than ω_r , the sense mode oscillates approximately in phase with the drive frequency. The design of an array of non-identical gyroscopes will involve choosing a Q for the sense axis that minimizes phase mismatch in the array and maximizes the amplitude response to the Coriolis driving force. The simulation results presented in the next section explore some of the tradeoffs in such a design.

3. SIMULATION RESULTS

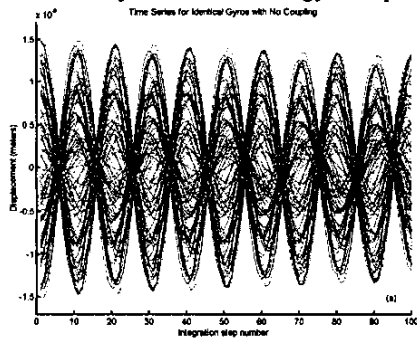
For all of the simulations an array of one hundred gyroscopes in a ten by ten two dimensional array was used. The mean values for the mass (m), linear restoring force ($k1$), damping (C), drive resonance (ω_r), applied angular rate (Ω), drive amplitude (A_d), and drive frequency (ω_d) are shown in table 1.

mass	1e-9	kg
K1	1	N/meter
C	3.1623e-7	N s/meter
ω_r	31623	rad/sec
Ω	0.175	rad/sec
A_d	10e-6	meters
ω_d	31623	rad/sec

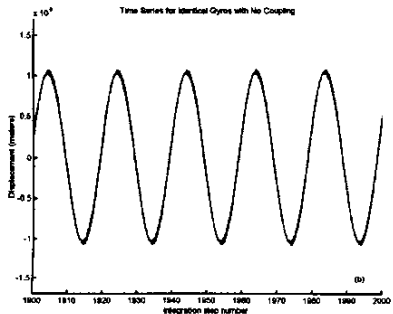
Table 1. Simulation Parameters with no variation

The simulations begin with an “ideal” case where the gyroscopes are identical and each gyroscope is driven exactly at w_d . After the initial plots, these constraints are removed and the mass is allowed to vary by $1e-9 \pm 2.5e-11$ kg with equal probability. This creates a variation in the resonant frequency of the drive axis of $5033\text{Hz} \pm 62.5$ Hz. For many of the simulations we will look at drive frequencies equal to the resonant frequency of the sense axis and at 4966 and 5100 Hz. There drive frequencies lie outside the maximum variation in the sense frequency introduced by varying the mass of the gyroscope by 2.5%. For all the simulations a random set of initial conditions was imposed on the system. The initial displacements of the sense mode for each gyroscope was randomly distributed between $0 \pm 1.5e-8$ meters with equal probability. The value of $1.5e-8$ is roughly the maximum displacement for a single gyroscope with the parameters given above. The sense mode was also given a random velocity between $0 \pm 1.0e-4$ meters/sec with equal probability. Initial velocities larger than this tended to destabilize the system. These random initial conditions place the array in very disordered state. These simulations do not reflect the expected performance of the gyroscopes. They were completed to explore and optimize the synchronization performance of the array of gyroscopes. A constant external angular rate of 0.175 rad/sec was applied in all simulations and the time for the summed displacements of each gyro to reach a constant amplitude was used to measure synchronization.

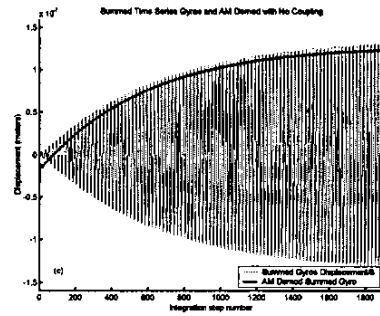
Figures 3a-c illustrate the initial conditions imposed on the array and the summed output and amplitude demodulated signal from the array of one hundred gyroscopes.



(3a)



(3b)



(3c)

Figure 3a-c. Time series and Demodulation. All figures use an ideal model with identical gyroscopes and drive frequency at resonance (5033Hz). 3(a) shows the effect of initial random conditions from $t=0$ to $t=100 \cdot T_s$, where $T_s = 20 \cdot 5e-7$ seconds. 3(b) shows the excellent phase and frequency synchronization from $t=1900 \cdot T_s$ to $2000 \cdot T_s$. 3(c) shows the increasing amplitude of the summed output from each gyroscope and the demodulated signal. This demodulation method is only possible for phase and frequency synchronized gyroscopes.

Figure 4 shows the results from an “ideal” system with identical gyroscopes and no variation in the drive frequency. A coupling term is also introduced in the model which has the form $\kappa \cdot (Z_{\text{neighbor}} - Z_{\text{self}})$ where Z is the sense mode displacement and κ is the coupling strength. A κ of zero corresponds to an uncoupled system. In the simulations, a nearest neighbor coupling method was employed. For gyroscopes in the center of the array the coupling term includes its four neighbors and the coupling for edge elements contains fewer terms.

The coupling term could be implemented in gyroscopes through a variable resistor connecting the sense axis capacitors of nearest neighbors in the array. The coupling term was modeling in these simulations to see if it improved the amplitude response or decreased the synchronization time for the summed gyro output signal. Figure 4 shows the effect of coupling on the ideal system with identical gyroscopes. No improvement in the amplitude response or synchronization time is achieved using coupling.

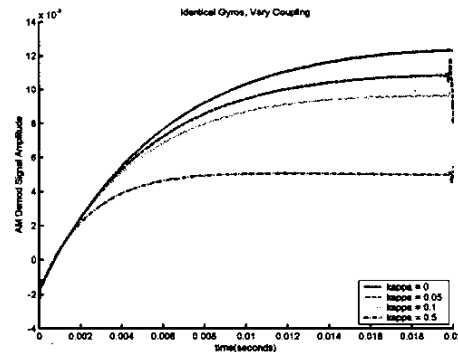


Figure 4. Identical Gyroscopes driven at resonance (5033 Hz). This plot shows that coupling decreases the amplitude response for an ideal array of gyroscopes.

In figure 5 a more realistic system that includes a random 2.5% variation in the mass is examined. This mass variation changes the resonant frequency of the sense mode between 5033 ± 62.5 Hz. This system now does not have a single resonant frequency to exploit. Three values for the drive frequency were chosen to examine the response of the array. They are at resonance, and slightly above and below the frequencies variation possible for the sense axis mode.

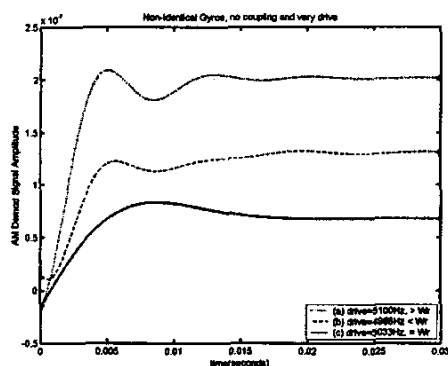


Figure 5. Non-Identical Gyroscopes and Effect of Drive Frequency.

The system driven at resonance now exhibits the worst amplitude and synchronization performance. This is due to the maximum slope change in the phase lag response near the mean resonance frequency (see figure 2). The best amplitude response is for a driving frequency above resonance (5100 Hz). This can be explained qualitatively by realizing that in this regime all the gyroscopes meet the condition $\omega_i < \omega_d$ and thus have approximately a π phase lag with respect to the drive frequency. This phase lag does not affect the demodulation of the summed output from the array since the gyroscopes are synchronized to the drive frequency with a constant phase lag.

In figure 6 a similar plot to figure 5 is done with the coupling strength kappa fixed at 0.1. This figure is very similar to the uncoupled system.

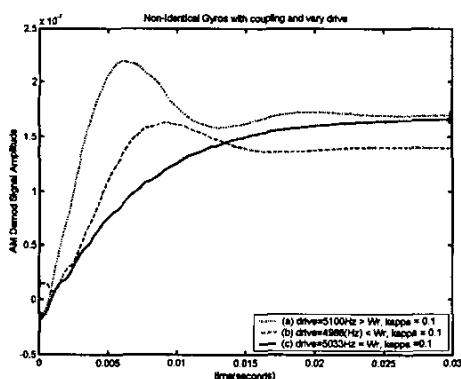


Figure 6. Non-Identical Gyroscopes and Effect of Drive Frequency

The effect of coupling does not change the general response of the array of gyroscopes but it does decrease the maximum amplitude of the summed gyroscope output signal. The final case that will be considered is minor variations in the drive frequency ω_d .

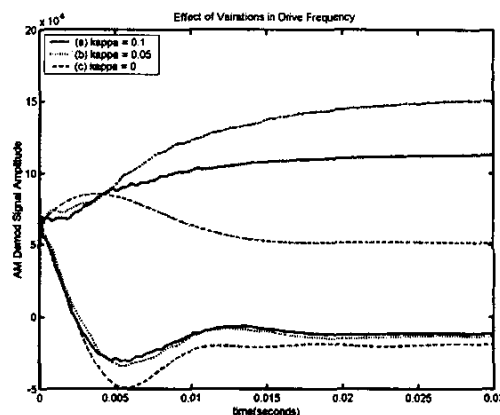


Figure 7. Non-Identical Gyros with Variation in Drive Frequency

The top three lines in figure 7 use a drive frequency equal to the mean resonance frequency of the array (5033Hz) and a variation in the drive axis of only 0.5 rad/sec. The lower three figures use a drive frequency greater than the mean sense resonant frequency and the variation in the drive is 12.5 rad/sec. In both cases the coupled system performs better than the uncoupled system.

4. SUMMARY

This paper demonstrates that for non-identical arrays of gyroscopes with variations in the drive frequency coupling can increase the synchronization in the array. The simulations and solutions for a single damped, driven harmonic oscillator also indicate that a driving frequency above the mean variation in resonant mode frequencies produces the greatest synchronization in the array. Future work will explore the effect of noise and a time varying angular velocity. It will also be necessary to characterize the response of the summed array displacement output to the applied angular velocity.

5. REFERENCES

- [1] Yazdi, N., Ayazi, F., Najafi, K. "Micromachined Inertial Sensors," *Proceeding of IEEE*, Vol. 86, No. 8, pp. 1640-1658, 1998
- [2] French, A.P., *Vibrations and Waves*, W.W. Norton and Company, England, 1971.